Surface Ligand Dynamics-Guided Preparation of Quantum Dots– Cellulose Composites for Light-Emitting Diodes

Ding Zhou,[†] Haoyang Zou,[†] Min Liu,[†] Kai Zhang,[†] Yu Sheng,*[,‡] Jianli Cui,*[,§] Hao Zhang,*[,†] and Bai Yang[†]

[†]State Key Laboratory of Supramolecular Structure and Materials, College of Chemistry, Jilin University, Changchun 130012, P. R. China

[‡]Department of Dermatology, First Affiliated Hospital, Harbin Medical University, Harbin 150001, P. R. China

[§]Department of Hand & Foot Surgery, The First Hospital of Jilin University, Changchun 130021, P. R. China

S *Supporting Information*

ABSTRACT: Surface ligand dynamics of colloidal quantum dots (QDs) has been revealed as an important issue for determining QDs performance in their synthesis and postsynthesis treatment, such as ligand-related photoluminescence, colloidal stability, and so forth. However, this issue is less associated with the preparation of highly luminescent nanocomposites, which usually leads to poor performance and repeatability. In this work, on the basis of the studies about surface ligand dynamics of aqueous QDs, highly luminescent QDs– cellulose composites are prepared and employed to fabricate high color purity light-emitting diodes (LEDs). Detailed investigations indicate that the species of QD capping ligands and in particular the temperature are the key for controlling the ligand dynamics. The preparation of nanocomposites using less dynamic ligand-modified

QDs at low temperature overcomes the conventional problems of QD aggregation, low QD content, luminescence quenching and shift, thus producing highly luminescent QDs–cellulose composites. This protocol is available for a variety of aqueous QDs, such as CdS, CdSe, CdTe, and CdSe$_x$Te$_{1-x}$, which permits the design and fabrication of QD-based LEDs using the nanocomposites as color conversion layer on a blue emitting InGaN chip.

KEYWORDS: *aqueous quantum dot, cellulose, white light-emitting diode, ligand dynamics, nanocomposites*
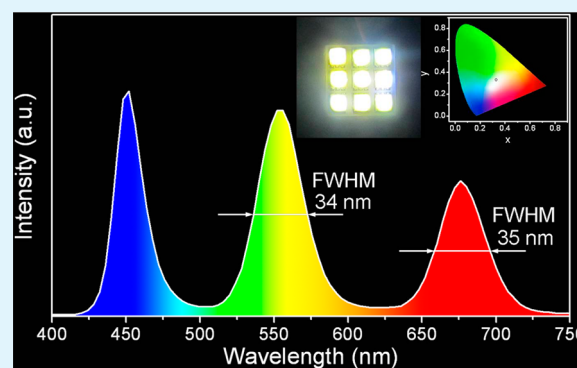
INTRODUCTION

With respect to the current illumination and display, the application of light-emitting diodes (LEDs) to achieve white light is overwhelming because of its low threshold voltage, low power, and high brightness.[1−8] The commercial white LEDs (WLEDs) are mainly made of blue light-emitting InGaN/GaN chip, and the color conversion layer composed of rare-earth phosphors.[9−11] The latter can partially convert the chip blue emission to yellow, thus generating apparent white light by combining the remaining blue emission and rare-earth yellow emission.[11,12] However, the color conversion using rare-earth phosphors usually generates broad emission, which leads to the harsh cool light of commercial WLEDs.[13] Consequently, the parameters of commercial WLEDs, such as Commission Internationale de l'Eclairage (CIE) chromaticity coordinates, color rendering index (CRI), correlated color temperature (CCT), and luminous efficacy, are hardly adjustable. For example, one of the most ideal display prototypes requires the coexistence of narrow blue, green, and red emission in WLEDs.[14−16] Despite green and red emission can be brought by using different rare-earth phosphors, the broad emission and unpredictable green-to-red energy transfer of rare-earth

mixtures shed doubt on further applications.[17] Associated with the low reserves of rare-earth elements, alternative materials are greatly welcome to improve the performance of WLEDs.[12]

Among various luminescent materials, quantum dots (QDs), also known as semiconductor nanocrystals, are competitive candidates in illumination and display, because of the narrow and tunable photoluminescence (PL), high PL quantum yields (PLQYs), broad excitation spectra, and good photostability.[18−29] In particular, the high color purity from the narrow emission of QDs is highly desired for the precise control of LED parameters, which cannot be achieved either using organic dyes or rare-earth phosphors. Although QDs possess these advantages, their LED application still meets several difficulties, including high cost, fluorescence deterioration, concentration quenching, as well as the fluorescent resonance energy transfer (FRET) between different QD components.[30] Note that the commonly used QDs are synthesized in organic media, which
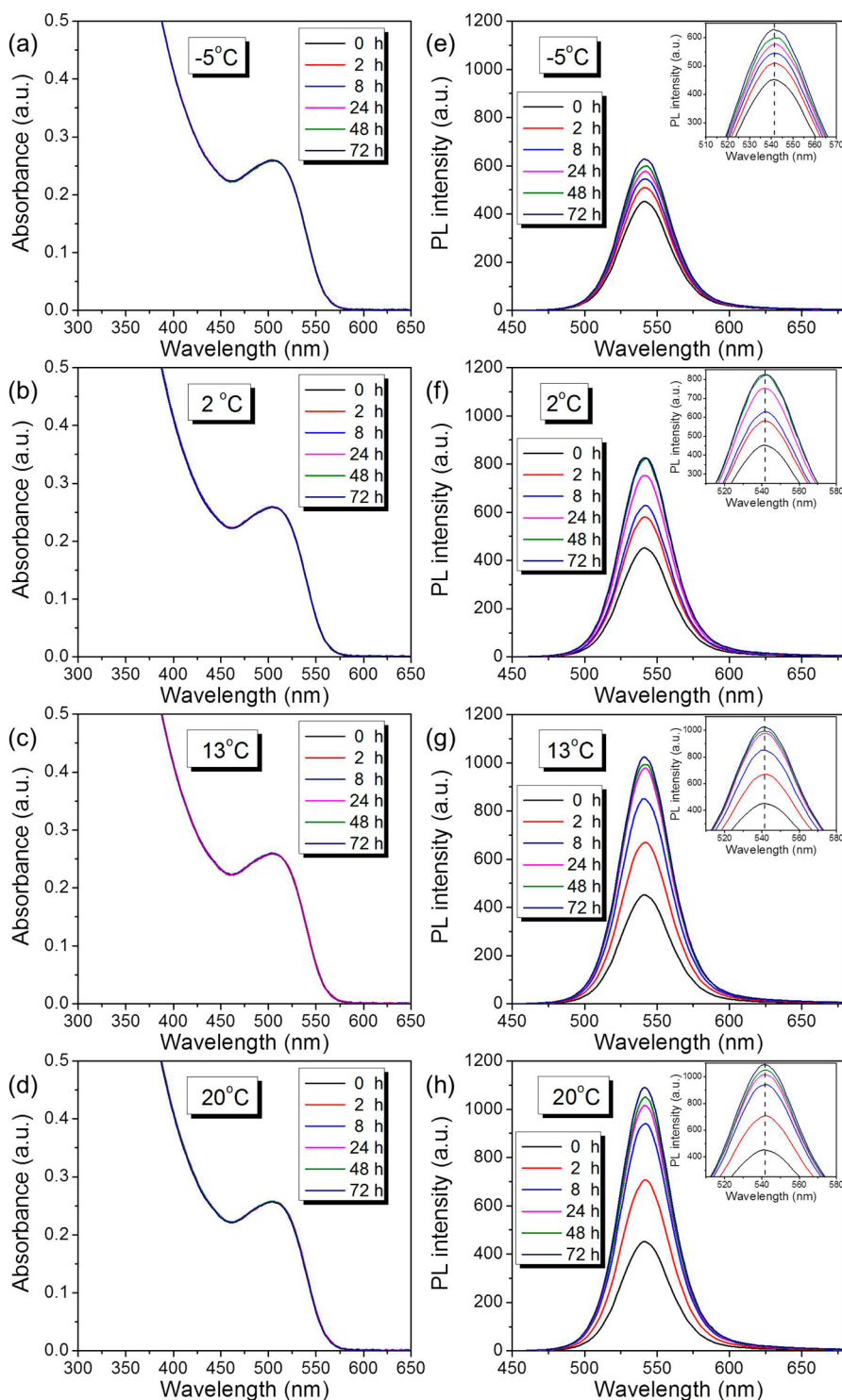
Figure 1. UV−vis absorption spectra (a−d), and PL emission spectra (e−h) of TGA-stabilized aqueous CdTe QDs as storing at −5 (a, e), 2 (b, f), 13 (c, g), and 20 °C (d, h) for specific duration.

possess lipophilic surfaces and are miscible with epoxy or silicone.[14,31−34] Despite the successes in constructing QD-based LEDs, this approach leads to several problems in commercial applications. First, the synthesis of QDs in organic media is very complicated, which requires waterless environment, high vacuum or N_2 protection, and high temperature over 250 °C.[35] Besides the high cost, the high energy consumption and high toxicity also lower the competitiveness for commercial LEDs. Second, the QD luminescence usually

deteriorates as packaged with lipophilic polymers, such as epoxy and silicone, during thermal curing, because the capping ligands and surface atoms of QDs are easy to be detached at elevated temperature.[36] Namely, the ligands are not stationary on the surface of QDs but dynamic in the surrounding media. This is also defined as surface ligand dynamics. Thus, the existence of QD ligand dynamics in fabricating nanocomposites usually leads to surface defects and QD aggregation. The former greatly reduces the PL intensity, while the latter leads to FRET and PL

quenching. So, although several methods are proposed to improve the compatibility of QDs with polymer media, the emission properties of QDs can hardly be fully maintained.[13,36−38] To promote the practical application of QD-based LEDs, novel approaches for fabricating QDs-polymer composites should be established by studying the surface ligand dynamics of colloidal QDs.

As the alternatives to the QDs synthesized in organic media, highly luminescent QDs can be also synthesized in water.[39−48] The current synthesis at room temperature already permits to produce aqueous QDs with low cost, large scale, and easy surface modification.[39] With respect to prepare QDs−polymer composites, the most facile protocol is to mix QDs with aqueous-processed polymers.[49] In this scenario, cellulose is a natural polymer, inherently exhibiting the advantages of ultralow cost, nontoxicity, easy processing, and so forth. However, the dissolution of natural cellulose in water should be operated in the presence of LiOH and $CO(NH_2)_2$. The mass fraction of LiOH or $CO(NH_2)_2$ is up to 24%.[50] The dissolving aqueous QDs in cellulose solution meet the challenge to increase QD concentration, because high QD content is required in fabricating LEDs. To increase QD content, it is better to dissolve cellulose in the aqueous mixtures of QDs, LiOH, and $CO(NH_2)_2$.[51] This in return meets the problem of QD surface ligand dynamics. In aqueous solution, the QD surface structure at any given instant of time is not static, because the surface ligands continually adsorb on or desorb from the surface.[52] Therefore, the ligands are dynamic rather than static, which are sensitive to the variation of surrounding media, such as ionic strength. Owing to the large amount of LiOH and $CO(NH_2)_2$, the high ionic strength accelerates the desorption of QD surface ligands and therewith leads to the obvious PL quenching and spectral redshift. To overcome this problem, the ligand dynamics of aqueous QDs in fabricating QDs−-cellulose composites should be well revealed.

In this paper, highly luminescent nanocomposites with controlled emission color and intensity are prepared from aqueous CdTe QDs and cellulose by studying the surface ligand dynamics of aqueous QDs and applied in fabricating tricolor LEDs. Detailed investigations reveal that the fabrication using less dynamic ligand-modified QDs at low temperature is capable to suppress surface ligands movement. Thus, QDs completely preserve the emission properties even in the solution with high LiOH and $CO(NH_2)_2$ concentration. The direct dissolution of cellulose in the aforementioned solution generates QDs−cellulose composite solution, which can be further solidified to produce practical nanocomposites. Owing to the additional saturation of QD surface dangling Cd bonds by the amine groups of $CO(NH_2)_2$, the emission intensity of the nanocomposites are greatly enhanced. The full width at half-maximum (fwhm) of the emission peaks of LEDs can be narrowed to less than 35 nm, showing the potential to achieve high color purity in tricolor display.

■ RESULTS AND DISCUSSION

Aqueous CdTe QDs that are stabilized by 1-thioglycerol (TG), thioglycolic acid (TGA), 3-mercaptopropionic acid (MPA), and 2-mercaptoethylamine (MA) are directly synthesized in water according to the Experimental Section. The as-synthesized QDs exhibit fine crystalline structure and controllable PL emission (Supporting Information, Figure S1 and S2). However, in the preparation of QDs−cellulose composites, the direct dissolution of LiOH and $CO(NH_2)_2$ in QD solution at room

temperature leads to serious PL quenching and spectral redshift. This variation may be caused by several factors, including QDs degradation, oxidation, photoinduced ligand dissociation, ligand dynamics, and so forth.[53−56] Even the preparation is operated in an airtight container and in the dark, obvious PL quenching and spectral redshift still exist. So, the PL variation should not relate with degradation, oxidation, and photoinduced ligand dissociation. According to our previous report,[55] ligand dynamics should be the main reason. To overcome this problem, the surface ligand dynamics of aqueous QDs is studied by altering the species of capping ligands, QD concentration, temperature, ionic strength, and so forth.

According to the surface functional groups, the capping ligands of aqueous CdTe QDs are divided into three types, including carboxyl (TGA and MPA), hydroxyl (TG), and amine (MA). In the current system, amine-functionalized CdTe QDs are not suitable for preparing QDs−cellulose composites, because they are unstable in the basic solution of LiOH and $CO(NH_2)_2$.[57] Only carboxyl- and hydroxyl-functionalized QDs are potentially available for fabricating composites. The PL stability of TGA-, MPA-, and TG-stabilized QD solution in the absence of LiOH and $CO(NH_2)_2$ is first compared at room temperature. It is found that the PL of TG-stabilized QDs is nearly unchanged during room temperature storage, whereas the PL variation of TGA-stabilized QDs is most obvious (Figures 1, S3, and S4). This phenomenon can be understood in terms of QDs surface optimization, which is closely associated with the ligand dynamics.[55] For the freshly synthesized QDs, though the surface sites of QDs are protected by ligands, some vacancies and defects still exist.[55] These defects can be further passivated during room temperature storage through the adsorption of excess cadmium-ligand complexes in the solution, which significantly enhances QDs PL.[55] The more dynamic the ligand is, the more rapid emission enhancement QDs indicate. As discussed in our previous work,[57] the two hydroxyl groups of TG are partially charged, which prevent the adsorption/desorption of their capped Cd, thus suppressing the ligand dynamics. In the case of TGA and MPA, different from the hydroxyl oxygen of TG, the carbonyl oxygen of TGA or MPA may further coordinate with the Cd in solution, thus accelerating ligand dynamics.[57] This reveals that TG is less dynamic than MPA and subsequent TGA as the capping ligand to stabilize aqueous QDs. From a different view, TGA-stabilized QDs are most suitable for investigating experiment variables-dependent surface ligand dynamics, because the dynamic adsorption/desorption of TGA is most rapid. Therefore, in the following discussions, TGA- and/or MPA-stabilized QDs are studied first to reveal the suitable temperature for suppressing ligand dynamics. Then, TG-stabilized CdTe QDs are investigated for producing QDs−cellulose composites.

The temperature-dependent ligand dynamics is studied by comparing the PL variation of TGA-stabilized CdTe QDs at −5, +2, +13, and +20 °C. −5 °C is adopted as the lowest temperature, because the QD solution will freeze below −5 °C. In general, the PL intensity of all QD solution increases as storing at different temperature, and the storage at high temperature leads to more obvious PL enhancement (Figures 1e−h and S3). As elevating to 40 °C, a faster PL enhancement is observed (Figure S5). Meanwhile, the PL peak positions and UV−vis absorption spectra are hardly changed, showing the unchanged QD size (Figure 1a−d). The XRD patterns are also similar, implying that the PL variation is not resulted from the
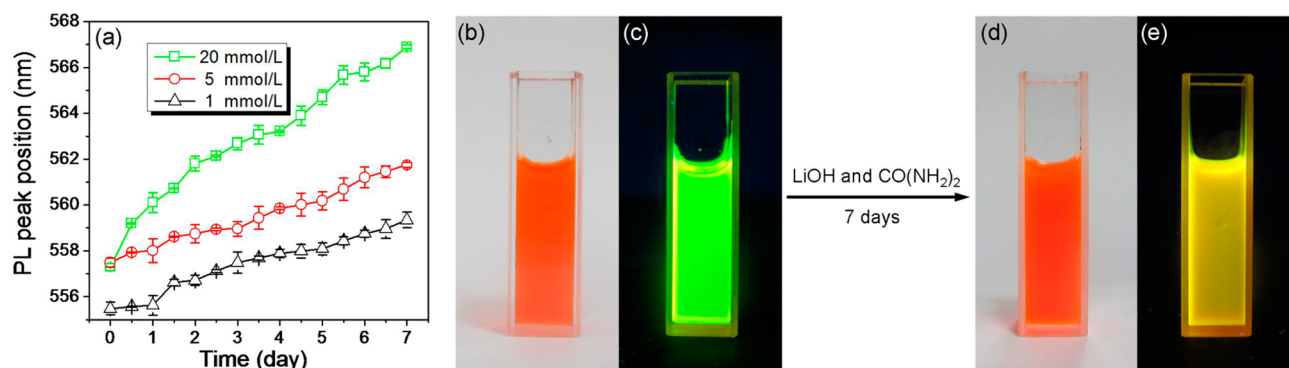
Figure 2. (a) Concentration-dependent variation of the PL peak positions of TG-stabilized CdTe QDs versus the storage duration at room temperature. The concentrations of QDs are 1, 5, and 20 mmol/L. The optical (b, d) and PL (c, e) photographs of the QD solutions as storing in the absence (b, c) and presence (d, e) of LiOH and $CO(NH_2)_2$ for 7 days.
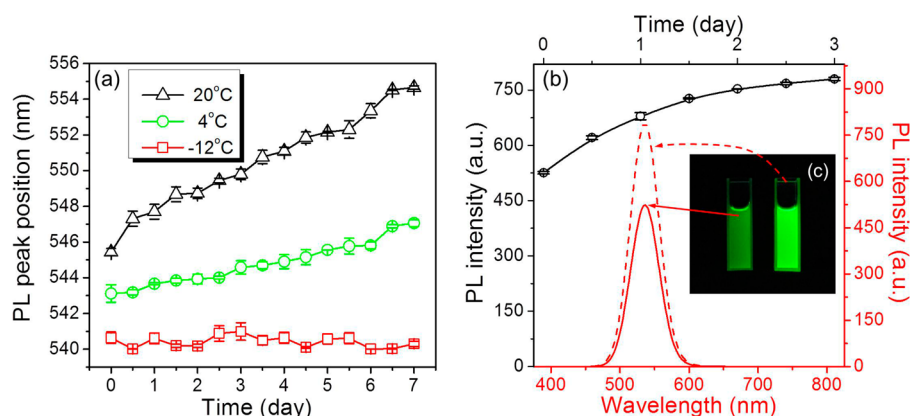

Figure 3. (a) Temperature-dependent variation of the PL peak positions of TG-stabilized CdTe QDs versus the storage duration. The concentration of QDs is 20 mM. (The black curve in b) Variation of the PL intensity of TG-stabilized CdTe QDs during the storage at −12 °C. PL spectra (red curve in b) and PL photographs (c) of the QD solution without (solid) and with (dash) storing in LiOH and $CO(NH_2)_2$ for 3 days.

alteration of composition and crystalline structure (Figure S6). Note that the XRD results are also compared with the standard XRD peaks of cubic CdS to exclude the formation CdS through possible ligand decomposition. It clearly indicates that no CdS forms during the storage. Furthermore, the XRD patterns of MPA- and TG-stabilized CdTe QDs with different storage duration at different temperature are supplied in Figure S7 and S8. For the same ligand, the XRD patterns are completely identical (Figure S6−S8), which further confirm the maintenance of crystalline structure during storage.

In general, the PL enhancement may result from two main aspects. One is the ligand dynamics, which can eliminate the traps on the surface of QDs, thus enhancing the emission. Another is the decomposition of ligands under light irradiation or heating treatment. This leads to the formation of CdS shell on the surface of CdTe QDs, and therewith enhances the PL emission.[56] However, once the QDs are synthesized, the XRD patterns do not change any longer during the storage at room temperature in the dark, which is clearly revealed by comparing the (220) diffraction peak (Figure S6−S8). These prove that the PL enhancement does not relate with ligand decomposition, because the room-temperature storage in the dark avoids the decomposition of ligands and the formation of CdS. So, the PL enhancement is solely attributed to the ligand dynamics at room temperature.[55] The coverage of TGA, MPA, and TG on QDs is calculated by combining elemental analysis. The coverage of different ligands on QDs is similar (~6.4 per

nm^2), indicating that the difference in PL variation does not lead from ligand-dependent coverage. So, the PL enhancement is reasonably assigned to QD surface optimization induced by ligand dynamics.[55] The dynamic adsorption/desorption of QD surface ligands reduces the surface dangling bonds by rebuilding the equilibrium of QD surface atomic structure. This strongly facilitates the exciton transition via radiative pathway, and therewith enhances the PL intensity.[56] High temperature promotes the ligand dynamics, thus enhancing the PL intensity more obviously. Temperature-dependent PL enhancement is also observed for MPA-stabilized CdTe QDs, but the variation is less obvious than TGA-stabilized QDs, because of the slower ligand dynamics (Figure S4). The aforementioned results clearly reveal that the surface ligands of aqueous QDs are less dynamic at lower temperature.

The effect of ionic strength on QD surface ligand dynamics is studied in the presence of LiOH and $CO(NH_2)_2$ with the consideration to fabricate QDs−cellulose composites. It is found that the PL of TG-, TGA-, and MPA-stabilized CdTe QD solutions exhibits obvious redshift after addition of LiOH and $CO(NH_2)_2$ and storage at room temperature. After 7 days' storage, the PL of 20 mM TG-stabilized QD solution indicates 10 nm redshift, while MPA- and TGA-stabilized QDs show 20 and 30 nm redshift (Figures 2 and S9). The redshift is attributed to the high ionic strength led from high LiOH and $CO(NH_2)_2$ concentration, which is around 4.6 M. The effect of LiOH and $CO(NH_2)_2$ concentrations on the PL shift of TG-

stabilized CdTe QDs is shown in Figure S10. With increasing LiOH and $CO(NH_2)_2$ concentration, the PL shift becomes more obvious, because the ionic strength is increased. Such condition promotes the aggregation and/or growth of QDs through the rapid diffusion of QD surface atoms and ligands.[58] In addition, the redshift becomes more obvious as increasing QD concentration (Figure 2a), because the local adsorption/desorption of ligands is more dynamic at high ionic strength.[58] The presence of high concentration LiOH and $CO(NH_2)_2$ decreases the freezing point of water. So, the ligand dynamics can be studied at lower temperature (Figure 3). At −12 °C, even storage in 4.6 M LiOH and $CO(NH_2)_2$ solution for 7 days, nearly no redshift of the PL of TG-stabilized CdTe QDs is observed. This means that the use of less dynamic ligand–modified QDs at low temperature is potentially capable of overcoming the emission variation in fabricating QDs−cellulose composites. Moreover, the PL intensity of TG-stabilized CdTe QDs enhances in the presence of LiOH and $CO(NH_2)_2$, because the surface dangling Cd bonds are further saturated by the amine-groups of $CO(NH_2)_2$ (Figure 3b,c).[59] Figure 3c exhibits the PL images of the QDs solution before and after addition of LiOH and $CO(NH_2)_2$ for 3 days. The absorbance of the solutions is identical for eliminating the deviation from concentration difference. So, it is safely concluded that the presence of LiOH and $CO(NH_2)_2$ leads to brighter PL.

In all, low temperature makes the adsorption/desorption of QD surface ligands less dynamic, and following the sequence of TGA, MPA, and TG, QD surface ligand dynamics becomes less obvious. Consequently, at −12 °C, TG-stabilized CdTe QDs are employed to fabricate QDs−cellulose composites. After dissolution of LiOH and $CO(NH_2)_2$, the TG-stabilized CdTe QDs aqueous solution is immediately cooled to −12 °C. Under vigorous stirring, cellulose is added to produce a QDs−cellulose composite solution, which is described in the Experimental Section. The composite solution has high viscosity and can be processed into various shapes after solidifying at room temperature (Figure 4). TEM image indicates that the QDs
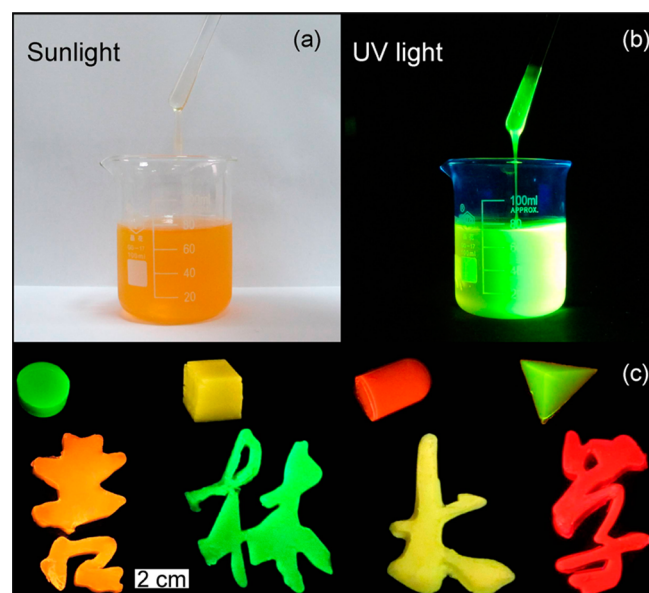

Figure 4. Photographs of QDs−cellulose composite solution under sunlight (a) and UV light (b). (c) PL images of QDs−cellulose composites in different shapes, which are excited by an ultraviolet lamp.

are well dispersed in a cellulose matrix by maintaining the original size (Figure S11). The composites preserve the size-dependent emission of the original aqueous CdTe QDs, which can be tuned from green to red (Figure 5). Compared with the
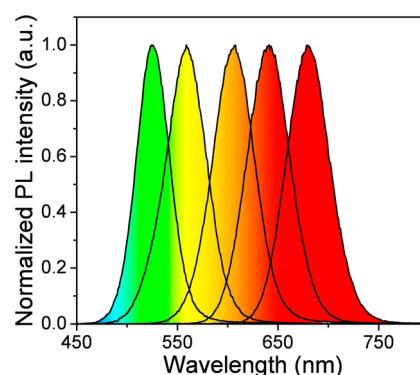

Figure 5. PL emission spectra of five QDs−cellulose composites with different emission colors. The diameters of QDs in QDs−cellulose composites are 2.3, 2.6, 3.1, 3.6, and 4.1 nm, respectively.

original QDs, the emission peak position and fwhm of QDs−cellulose composites are nearly unchanged. In contrast, when TGA-stabilized CdTe QDs are selected for preparing QDs−cellulose composites, the PL emission of the resultant composites shows clear redshift (Figure S12). This means that TGA-stabilized QDs are not suitable for fabricating composites. In addition, the PLQYs of solidified composites from TG-stabilized CdTe QDs are up to 33% (Table 1),

Table 1. PLQYs and FWHM of QDs−Cellulose Composites

PL peak position (nm)	520	560	600	640	680
PLQYs of composites (%)	18	33	31	28	19
fwhm (nm)	38	47	48	49	49

comparable to the previously reported composites.[16] The QDs−cellulose composites can be purified by removing LiOH and $CO(NH_2)_2$ through dialysis, which is proved by Fourier transform infrared (FTIR) spectra and elemental analysis (Figure S13). However such purification is not necessary in practical applications, because the presence of LiOH and $CO(NH_2)_2$ does not damage the performance of QDs−cellulose composites. Instead, the presence of $CO(NH_2)_2$ greatly enhances the PL of composites by saturating QD surface dangling Cd atoms.

The solidified composites possess compact structure, which is confirmed by SEM observation (Figure S14). This improves the stability of as-prepared composites. The composites exhibit excellent photostability. Figure 6 compares the PL spectra of QDs−cellulose composites before and after three months' sunlight irradiation in air. The PL peak position and PLQYs are unchanged. Whereas, obvious blue shift and intensity decrease of the PL spectra of aqueous CdTe QDs is found only after 3 days' sunlight irradiation, showing the serious photogenerated QD decomposition.[60] The composites indicate good thermal stability. Thermogravimetric analysis data reveals that when the temperature is lower than 100 °C, no weight loss occurs because of the embedment of QDs in cellulose (Figure S15).[51] The low temperature resistance of QDs−cellulose composites is tested in liquid nitrogen (Figure S16). No emission variation is observed by immersing the composites in liquid nitrogen and
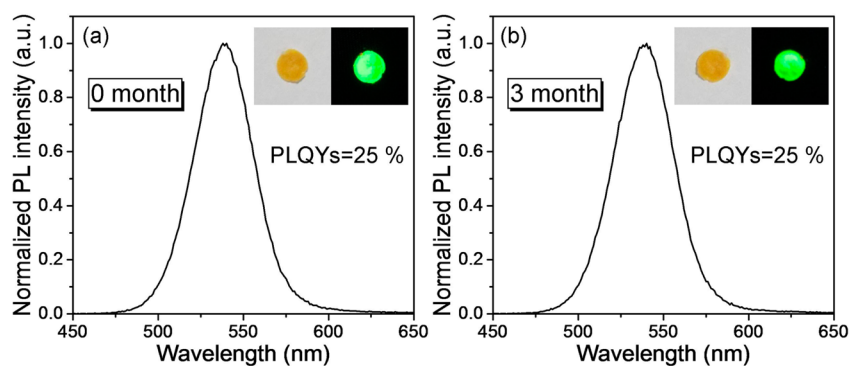
Figure 6. PL spectra and PLQYs of QDs−cellulose composites before (a) and after (b) 3 months of sunlight irradiation. The insets in (a, b) are the photographs taken under sunlight and UV light.
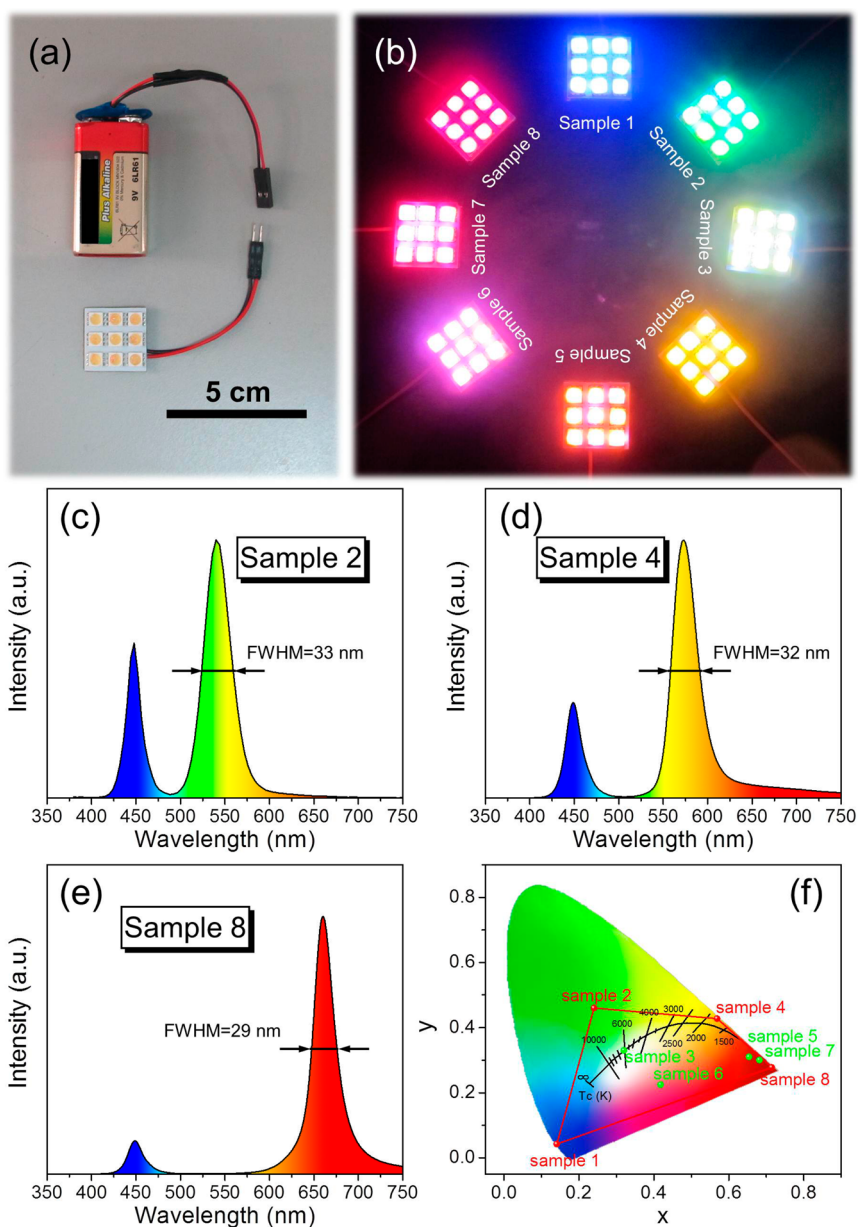

Figure 7. (a) Area light composed of nine WLED devices and a 9 V battery. (b) The photograph of eight LED area lights with different emission. (c−e) The emission spectra of samples 2, 4, and 8. (f) CIE chromaticity diagram showing the (x,y) color coordinates of the eight LED lights. The black curve represents the variation of color temperature with the color coordinates. The points on the black straight line are constant color temperature.
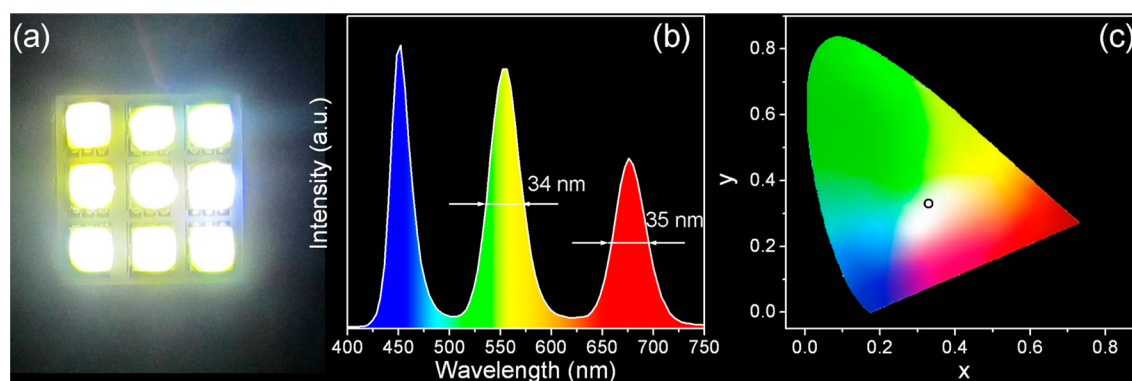
Figure 8. (a) Photograph of WLED area light source. Corresponding emission spectrum (b), and color coordinate (c) of the WLED are also shown.

returning to room temperature. To test the long-term stability of composites, the PL of QDs−cellulose composites is compared by storing at +20 and −12 °C for 3 days. No discrepancies are found in PL emission (Figure S17). Owing to the lipophobicity of cellulose, the composites also resist organic solvents (Figure S18). It means that although the composites are not hydrophobic, a layer of hydrophobic polymers can be further coated to isolate air for practical LED applications.

In addition, the ligand dynamics-guided preparation permits to produce CdTe QDs−cellulose composites in controlled manner. Besides the emission color (Figure 5 and Table 1), the concentration of QDs in composites can be also tuned from 0 to 10 wt % by altering the content of QDs in composite solution. As a result, the emission intensity is controllable (Figure S19). Such method is extendable to other QDs, such as CdS, CdSe, and $CdSe_xTe_{1−x}$, thus broadening the spectral range of luminescent composites (Figure S20). These advantages make the QDs−cellulose composites potentially applicable as the color conversion layer for LEDs.

In fabricating LEDs, the QDs−cellulose composite solution is deposited on commercially available 0.2 W InGaN LED chip, and solidified at room temperature for 5 h (Figure S21a). To better display the performance and eliminate local overexposure originated from point light source, nine LED devices are connected to fabricate 3 × 3 area lights (Figure S21b). Depending on the emission of QDs−cellulose composites, the area lights with different emission colors are obtained (Figure 7a and b). It should be mentioned that the fwhm of LED emission becomes narrower as the concentration of QDs is enhanced in the color conversion layer. For example, the PL fwhm of QD aqueous solution with green, yellow, and red emission is narrowed from 38, 47, and 49 nm to 33, 32, and 29 nm in the final LEDs (Figure 7c−e). This reveals the high color purity of LED emission, which is comparable to the high-quality QDs synthesized in organic media. The reason for emission narrowing is attributed to the reabsorption of QD emission in the composites with high QD concentration and long optical path. As mentioned in our previous work, the emission from smaller QDs in the QD ensemble can be readsorbed by the larger ones, thus leading to spectral redshift and narrowing.[61] To confirm the influence of optical path, two QDs−cellulose composites with same QD concentration but different thickness are prepared. For emitting the composites, the light source and detector are placed on the same sides or different sides of the composites, which leads to a different optical path (Figure S22). On the same sides, the measured emission is from the reflection of composites, which shortens

the path of light transmission and suppresses emission reabsorption. On the different sides, the path of light transmission is through the composites, thus the reabsorption of QD emission is inevitable. The influence on the apparent PL emission of thick composites is more obvious than that of thin composites. The thicker the composites are, the narrower the PL spectra are (Figure S23). These results clearly indicate that the emission reabsorption becomes stronger as increasing the length of the optical path. In LEDs, the InGaN chip and emission detector are placed on different sides of composites. The thickness of the composites is around 0.2 cm. So, the PL narrowing is evident.

The CIE color coordinates of eight LED devices are presented in Figure 7f. The outline color coordinates of the LEDs are (0.71, 0.28), (0.57, 0.43), (0.24, 0.46), and (0.14, 0.04). Based on the theory of colorimetry,[14] the LEDs with any emission colors in the quadrangle can be obtained by mixing the composites with different emission colors. The area of the quadrangle nearly covers the black curve, which represents the variation of CCT with the color coordinates (Figure 7f). This means that the CCT of LEDs is tunable from 1500 to tens of thousands degrees Kelvin, including the CCT from the poles to the equator. By combining the 557 nm yellow emission of QDs−cellulose composites and the 450 nm emission of InGaN chip, the capability to fabricate the area light source with white emission is demonstrated (Figure 7b, sample 3).

To fabricate high performance WLEDs with specific applications in illumination and display, for example tricolor display, the capability to fabricate WLEDs from multiple QD components is tested by combining the green and red emission of QDs−cellulose composites and the blue emission of InGaN chip. However, the direct blending of QDs with different emission colors leads to serious FRET from green-emitting QDs to red-emitting ones, making the apparent emission of final LED uncontrollable.[17] To overcome this problem, a gradient deposition of two QDs−cellulose composites respectively with 670 and 550 nm emission on InGaN chip is performed (Figure 8). Because the red-emitting composites are first excited by InGaN chip, and then green-emitting ones, the green-to-red FRET is efficiently avoided. Thus, it is capable to tune the intensity of blue, green, and red emission peaks in controlled manner. The fwhm of all three peaks are narrower than 35 nm. The high color purity of the WLEDs shows the potential in tricolor display.

■ CONCLUSIONS

In summary, QDs−cellulose composites are fabricated by studying the surface ligand dynamics of aqueous QDs and applied as the color conversion layer to fabricate LEDs. Detailed investigations demonstrate that the dynamic adsorption/desorption of QD surface ligands is suppressed using less dynamic capping ligands at low temperature. The favorable condition to produce QDs−cellulose composites with strong PL emission is the fabrication using TG-stabilized QDs at −12 °C. The as-prepared QDs−cellulose composites possess narrow fwhm, excellent stability, high PLQYs, tunable composition and emission color, which permit LEDs to be fabricated with high color purity and controllable emission color. As an example, a WLED for tricolor display is demonstrated.

■ EXPERIMENTAL SECTION

Materials. Tellurium powder (∼200 mesh, 99.8%), 3-mercapto-propionic acid (MPA, 99+%), thioglycolic acid (TGA, 98%), 2-mercaptoethylamine (MA), and 1-thioglycerol (TG, 98%) were purchased from Aldrich. NaBH$_4$ (96%), NaOH (98%), LiOH (98%), CO(NH$_2$)$_2$ (99%), Na$_2$TeO$_3$ (98+%), CdCl$_2$ (99%), 2-propanol (99%), and N$_2$H$_4$·H$_2$O (80%) were commercially available products and used as received. The cellulose samples (cotton linter pulps) were supplied by Hubei Chemical Fiber Co. Ltd. (Xiangfan, China). The weight-average molecular weight (M_w) of cellulose was 9.2×10^4.[50]

Synthesis of TGA- and MPA-Stabilized Aqueous CdTe QDs and the Ligand Dynamics. TGA- and MPA-stabilized CdTe QDs were synthesized according to our previous method.[62] Typically, TGA-stabilized CdTe precursors were foremost synthesized by injecting freshly prepared NaHTe aqueous solution into N$_2$-saturated CdCl$_2$ solution at pH 9.5 in the presence of TGA. The concentration of precursors was 20 mM referring to Cd^{2+}. The molar ratio of Cd^{2+}/MPA/HTe$^-$ was 1:2.4:0.2. To obtain the QDs with desired emission color, the precursor solutions were refluxed at 100 °C with specific duration to maintain QD growth. Following a similar procedure, except using MPA as the capping ligand, MPA-stabilized CdTe QDs were prepared.

In the investigation of surface ligand dynamics, freshly synthesized TGA-stabilized CdTe QDs were divided into four equal intervals, which were stored at −5, +2, +13, and +20 °C. For MPA-stabilized CdTe QDs, the QD solution was divided into two equal intervals and stored at −5, and 20 °C. After storing these intervals with specific duration, the PL emission and UV−vis absorption spectra were measured for monitoring the variation of QDs.

Room-Temperature Synthesis of TG-Stabilized Aqueous CdTe QDs and the Ligand Dynamics in the Solution with High Ionic Strength. TG-stabilized CdTe QDs were synthesized through a one-pot hydrazine-promoted method at room temperature.[39] Typically, 4 mL of 100 mM CdCl$_2$ aqueous solution, 58 mL of water, 85 μL of TG, 4 mL of 20 mM Na$_2$TeO$_3$ aqueous solution, 50 mg of NaBH$_4$, and 10 mL of 80% N$_2$H$_4$·H$_2$O were added in a conical flask in turn. The concentration of QDs was 5 mM referring to Cd^{2+}, and the molar ratio of Cd^{2+}/TG/TeO$_3$$^{2-}$/NaBH$_4$ was 1:2.4:0.2:3.4. Then, the mixture was stored at room temperature to maintain the growth of QDs. The emission colors could be tunable from 510 to 650 nm by altering the storage duration. The as-synthesized QDs were purified by adding 2-propanol to QDs solution and centrifugation for removing N$_2$H$_4$·H$_2$O. The precipitates of QDs were dissolved in a pH 9.5 aqueous solution containing Cd^{2+} and TG. To investigate the ligand dynamics, 0.22 g of LiOH and 0.42 g of CO(NH$_2$)$_2$ were added into 2 mL of TG-stabilized CdTe QDs solution. The mixture was stored at −12 and +20 °C with specific duration. PL emission spectra were measured for monitoring the variation of QDs.

Preparation of QDs−Cellulose Composites. 2 mL of 20 mM TG-stabilized CdTe QDs synthesized at room temperature, 0.22 g of LiOH, and 0.42 g of CO(NH$_2$)$_2$ were mixed, and immediately cooled to −12 °C. After rapidly adding 0.16 g of cellulose, the mixture was

stirring for 2 min to achieve QDs−cellulose composite solution. The composite solution was poured into the models with various shapes, and then solidified at room temperature within 5 h.

Fabrication of LEDs from QDs−Cellulose Composites. InGaN LED chips without phosphor coating were purchased from Shen Zhen Hongcai Elecronics CO., Ltd. The microchip was placed on the bottom of the LED base. The emission of the LED chip was centered at 450 nm, and the operating voltage was 3.0 V. The two leads on LED were prepared to connect with the power supply. In the fabrication of color conversion layer, QDs−cellulose composite solutions with different emission colors were filled into the cup-shaped void of LED chip (Figure S21a). After solidified at room temperature within 5 h, the LEDs from QDs−cellulose composites were fabricated.

Characterization. PL spectroscopy was performed with a Shimadzu RF-5301 PC spectrophotometer. The excitation wavelength was 400 nm. UV−visible absorption spectra were obtained using a Lambda 800 UV−vis spectrophotometer. Transmission electron microscopy (TEM) was conducted using a Hitachi H-800 electron microscope at an acceleration voltage of 200 kV with a CCD camera. Scanning electron microscope (SEM) image was taken with a JEOL FESEM 6700F electron microscope with primary electron energy of 3 kV. Thermogravimetric analysis was measured on an American TA Q500 analyzer under N$_2$ atmosphere with the flow rate of 100 mL·min^{-1}. Fourier transform infrared (FTIR) spectra were performed with a Nicolet AVATAR 360 FTIR instrument. Inductive coupled plasma emission spectrometer (ICP) was carried out with PERKIN ELMER OPTIMA 3300DV analyzer. X-ray powder diffraction (XRD) investigation was carried out using Siemens D5005 diffractometer. The color of light was identified by the CIE (Commission Internationale de L'Eclairage 1931) colorimetry system. Any color could be described by the chromaticity (x, y) coordinates on the CIE diagram. The absolute PLQYs of QDs−cellulose composites were measured on Edinburgh FLS920 (excited at 400 nm) equipped with an integrating sphere. Before the measurement, the instrument was calibrated by the quinine in 0.5 M H$_2$SO$_4$ aqueous solution, where the final concentration was 1×10^{-5} M to eliminate the concentration quenching. The measured PLQY of quinine was demonstrated to be equal to the real one. Then, the blank laser excitation line of 400 nm was measured first. Then, the sample was placed on the sample holder in the integrating sphere for the measurements of the emission spectra. Finally, the QYs were calculated according to the previous paper with the software supplied by the manufacturer. The spectra and brightness-current density−voltage characteristics of the LEDs were measured by combining a Spectrascan PR-650 spectrophotometer with an integral sphere and a computer-controlled direct-current power supply Keithley model 2400 voltage−current source under ambient condition at room temperature.

■ ASSOCIATED CONTENT

⑤ Supporting Information

The characterization of aqueous CdTe QDs and QDs−cellulose composites, the ligand dynamics of TGA- and MPA-stabilized CdTe QDs in the presence of LiOH and CO(NH$_2$)$_2$, the stability of QDs−cellulose composites, and the influence of optical path on PL fwhm. The Supporting Information is available free of charge on the ACS Publications website at DOI: 10.1021/acsami.5b03004.

■ AUTHOR INFORMATION

Corresponding Authors

*Fax: +86 431 85193423. E-mail: sf555812@163.com.
*E-mail: tsuijianli@126.com.
*E-mail: hao_zhang@jlu.edu.cn.

Author Contributions

The manuscript was written through contributions of all authors. All authors have given approval to the final version of the manuscript.

Notes

ACKNOWLEDGMENTS

REFERENCES

(1) Dai, X. L.; Zhang, Z. X.; Jin, Y. Z.; Niu, Y.; Cao, H. J.; Liang, X. Y.; Chen, L. W.; Wang, J. P.; Peng, X. G. Solution-Processed, High-Performance Light-Emitting Diodes Based on Quantum Dots. *Nature* **2014**, *515*, 96−99.

(2) Mashford, B. S.; Stevenson, M.; Popovic, Z.; Hamilton, C.; Zhou, Z. Q.; Breen, C.; Steckel, J.; Bulovic, V.; Bawendi, M.; Coe-Sullivan, S.; Kazlas, P. T. High-Efficiency Quantum-Dot Light-Emitting Devices with Enhanced Charge Injection. *Nat. Photonics* **2013**, *7*, 407−412.

(3) Taniyasu, Y.; Kasu, M.; Makimoto, T. An Aluminium Nitride Light-Emitting Diode with a Wavelength of 210 Nanometres. *Nature* **2006**, *441*, 325−328.

(4) Tsukazaki, A.; Ohtomo, A.; Onuma, T.; Ohtani, M.; Makino, T.; Sumiya, M.; Ohtani, K.; Chichibu, S. F.; Fuke, S.; Segawa, Y.; Ohno, H.; Koinuma, H.; Kawasaki, M. Repeated Temperature Modulation Epitaxy for p-Type Doping and Light-Emitting Diode Based on ZnO. *Nat. Mater.* **2004**, *4*, 42−46.

(5) Colvin, V. L.; Schlamp, M. C.; Alivisatos, A. P. Light-Emitting Diodes Made from Cadmium Selenide Nanocrystals and a Semiconducting Polymer. *Nature* **1994**, *370*, 354−357.

(6) Kim, B. H.; Onses, M. S.; Lim, J. B.; Nam, S.; Oh, N.; Kim, H.; Yu, K. J.; Lee, J. W.; Kim, J. H.; Kang, S. K.; Lee, C. H.; Lee, J.; Shin, J. H.; Kim, N. H.; Leal, C.; Shim, M.; Rogers, J. A. High-Resolution Patterns of Quantum Dots Formed by Electrohydrodynamic Jet Printing for Light-Emitting Diodes. *Nano Lett.* **2015**, *15*, 969−973.

(7) Shen, H. B.; Cao, W. R.; Shewmon, N. T.; Yang, C. C.; Li, L. S.; Xue, J. G. High-Efficiency, Low Turn-on Voltage Blue-Violet Quantum-Dot-Based Light-Emitting Diodes. *Nano Lett.* **2015**, *15*, 1211−1216.

(8) Li, X. M.; Liu, Y. L.; Song, X. F.; Wang, H.; Gu, H. S.; Zeng, H. B. Intercrossed Carbon Nanorings with Pure Surface States as Low-Cost and Environment-Friendly Phosphors for White-Light-Emitting Diodes. *Angew. Chem., Int. Ed.* **2015**, *54*, 1759−1764.

(9) Lee, S.; Hong, J. Y.; Jang, J. Multifunctional Graphene Sheets Embedded in Silicone Encapsulant for Superior Performance of Light-Emitting Diodes. *ACS Nano* **2013**, *7*, 5784−5790.

(10) Otto, T.; Müller, M.; Mundra, P.; Lesnyak, V.; Demir, H. V.; Gaponik, N.; Eychmüller, A. Colloidal Nanocrystals Embedded in Macrocrystals: Robustness, Photostability, and Color Purity. *Nano Lett.* **2012**, *12*, 5348−5354.

(11) Li, X. F.; Budai, J. D.; Liu, F.; Howe, J. Y.; Zhang, J. H.; Wang, X. J.; Gu, Z. J.; Sun, C. J.; Meltzer, R. S.; Pan, Z. W. New Yellow Ba$_{0.93}$Eu$_{0.07}$Al$_2$O$_4$ Phosphor for Warm-White Light-Emitting Diodes through Single-Emitting-Center Conversion. *Light: Sci. Appl.* **2013**, *2*, e50.

(12) Dai, Q. Q.; Duty, C. E.; Hu, M. Z. Semiconductor-Nanocrystals-Based White Light-Emitting Diodes. *Small* **2010**, *6*, 1577−1588.

(13) Liang, R. Z.; Yan, D. P.; Tian, R.; Yu, X. J.; Shi, W. Y.; Li, C. Y.; Wei, M.; Evans, D. G.; Duan, X. Quantum Dots-Based Flexible Films and Their Application as the Phosphor in White Light-Emitting Diodes. *Chem. Mater.* **2014**, *26*, 2595−2600.

(14) Jang, E.; Jun, S.; Jang, H.; Lim, J.; Kim, B.; Kim, Y. White-Light-Emitting Diodes with Quantum Dot Color Converters for Display Backlights. *Adv. Mater.* **2010**, *22*, 3076−3080.

(15) Guo, X.; Wang, C. F.; Yu, Z. Y.; Chen, L.; Chen, S. Facile Access to Versatile Fluorescent Carbon Dots toward Light-Emitting Diodes. *Chem. Commun.* **2012**, *48*, 2692−2694.

(16) Demir, H. V.; Nizamoglu, S.; Erdem, T.; Mutlugun, E.; Gaponik, N.; Eychmüller, A. Quantum Dot Integrated LEDs Using Photonic and Excitonic Color Conversion. *Nano Today* **2011**, *6*, 632−647.

(17) Wang, X. B.; Yan, X. S.; Li, W. W.; Sun, K. Doped Quantum Dots for White-Light-Emitting Diodes without Reabsorption of Multiphase Phosphors. *Adv. Mater.* **2012**, *24*, 2742−2747.

(18) Murray, C. B.; Norris, D. J.; Bawendi, M. G. Synthesis and Characterization of Nearly Monodisperse CdE (E = S, Se, Te) Semiconductor Nanocrystallites. *J. Am. Chem. Soc.* **1993**, *115*, 8706−8715.

(19) Cao, Y. W.; Banin, U. Growth and Properties of Semiconductor Core/Shell Nanocrystals with InAs Cores. *J. Am. Chem. Soc.* **2000**, *122*, 9692−9702.

(20) Tang, K. B.; Qian, Y. T.; Zeng, J. H.; Yang, X. G. Solvothermal Route to Semiconductor Nanowires. *Adv. Mater.* **2003**, *15*, 448−450.

(21) Nedeljković, J. M.; Mićić, O. I.; Ahrenkiel, S. P.; Miedaner, A.; Nozik, A. J. Growth of InP Nanostructures via Reaction of Indium Droplets with Phosphide Ions: Synthesis of InP Quantum Rods and Inp-TiO$_2$ Composites. *J. Am. Chem. Soc.* **2004**, *126*, 2632−2639.

(22) Pang, Q.; Zhao, L. J.; Cai, Y.; Nguyen, D. P.; Regnault, N.; Wang, N.; Yang, S. H.; Ge, W. K.; Ferreira, R.; Bastard, G.; Wang, J. N. CdSe Nano-Tetrapods: Controllable Synthesis, Structure Analysis, and Electronic and Optical Properties. *Chem. Mater.* **2005**, *17*, 5263−5267.

(23) Zheng, Y. G.; Gao, S. J.; Ying, J. Y. Synthesis and Cell-Imaging Applications of Glutathione-Capped CdTe Quantum Dots. *Adv. Mater.* **2007**, *19*, 376−380.

(24) Ouyang, J. Y.; Zaman, M. B.; Yan, F. J.; Johnston, D.; Li, G.; Wu, X. H.; Leek, D.; Ratcliffe, C. I.; Ripmeester, J. A.; Yu, K. Multiple Families of Magic-Sized CdSe Nanocrystals with Strong Bandgap Photoluminescence via Noninjection One-Pot Syntheses. *J. Phys. Chem. C* **2008**, *112*, 13805−13811.

(25) Zou, L.; Gu, Z. Y.; Zhang, N.; Zhang, Y. L.; Fang, Z.; Zhu, W. H.; Zhong, X. H. Ultrafast Synthesis of Highly Luminescent Green- to Near Infrared-Emitting CdTe Nanocrystals in Aqueous Phase. *J. Mater. Chem.* **2008**, *18*, 2807−2815.

(26) Xia, Y. S.; Tang, Z. Y. Monodisperse Hollow Supraparticles via Selective Oxidation. *Adv. Funct. Mater.* **2012**, *22*, 2585−2593.

(27) Shieh, F.; Saunders, A. E.; Korgel, B. A. General Shape Control of Colloidal CdS, CdSe, CdTe Quantum Rods and Quantum Rod Heterostructures. *J. Phys. Chem. B* **2005**, *109*, 8538−8542.

(28) Wang, X.; Zhuang, J.; Peng, Q.; Li, Y. D. A General Strategy for Nanocrystal Synthesis. *Nature* **2005**, *437*, 121−124.

(29) Xie, R. G.; Kolb, U.; Basché, T. Design and Synthesis of Colloidal Nanocrystal Heterostructures with Tetrapod Morphology. *Small* **2006**, *2*, 1454−1457.

(30) Clapp, A. R.; Medintz, I. L.; Mauro, J. M.; Fisher, B. R.; Bawendi, M. G.; Mattoussi, H. Fluorescence Resonance Energy Transfer between Quantum Dot Donors and Dye-Labeled Protein Acceptors. *J. Am. Chem. Soc.* **2004**, *126*, 301−310.

(31) Jun, S.; Lee, J.; Jang, E. Highly Luminescent and Photostable Quantum Dot-Silica Monolith and Its Application to Light-Emitting Diodes. *ACS Nano* **2013**, *7*, 1472−1477.

(32) Kim, S.; Kim, T.; Kang, M.; Kwak, S. K.; Yoo, T. W.; Park, L. S.; Yang, I.; Hwang, S.; Lee, J. E.; Kim, S. K.; Kim, S. Highly Luminescent InP/GaP/ZnS Nanocrystals and Their Application to White Light-Emitting Diodes. *J. Am. Chem. Soc.* **2012**, *134*, 3804−3809.

(33) Kim, K.; Woo, J. Y.; Jeong, S.; Han, C. S. Photoenhancement of a Quantum Dot Nanocomposite via UV Annealing and Its Application to White LEDs. *Adv. Mater.* **2011**, *23*, 911−914.

(34) Yang, X. Y.; Dev, K.; Wang, J. X.; Mutlugun, E.; Dang, C.; Zhao, Y. B.; Liu, S. W.; Tang, Y. X.; Tan, S. T.; Sun, X. W.; Demir, H. V. Light Extraction Efficiency Enhancement of Colloidal Quantum Dot Light-Emitting Diodes Using Large-Scale Nanopillar Arrays. *Adv. Funct. Mater.* **2014**, *24*, 5977−5984.

(35) Qu, L. H.; Peng, X. G. Control of Photoluminescence Properties of CdSe Nanocrystals in Growth. *J. Am. Chem. Soc.* **2002**, *124*, 2049−2055.

(36) Lee, J.; Sundar, V. C.; Heine, J. R.; Bawendi, M. G.; Jensen, K. F. Full Color Emission from II-VI Semiconductor Quantum Dot-Polymer Composites. *Adv. Mater.* **2000**, *12*, 1102−1105.

(37) Selvan, S. T.; Patra, P. K.; Ang, C. Y.; Ying, J. Y. Synthesis of Silica-Coated Semiconductor and Magnetic Quantum Dots and Their Use in the Imaging of Live Cells. *Angew. Chem., Int. Ed.* **2007**, *46*, 2448−2452.

(38) Chan, Y.; Snee, P. T.; Caruge, J. M.; Yen, B. K.; Nair, G. P.; Nocera, D. G.; Bawendi, M. G. A Solvent-Stable Nanocrystal-Silica Composite Laser. *J. Am. Chem. Soc.* **2006**, *128*, 3146−3147.

(39) Zhou, D.; Lin, M.; Chen, Z. L.; Sun, H. Z.; Zhang, H.; Sun, H. C.; Yang, B. Simple Synthesis of Highly Luminescent Water-Soluble CdTe Quantum Dots with Controllable Surface Functionality. *Chem. Mater.* **2011**, *23*, 4857−4862.

(40) Guo, J.; Yang, W. L.; Wang, C. C. Systematic Study of the Photoluminescence Dependence of Thiol-Capped CdTe Nanocrystals on the Reaction Conditions. *J. Phys. Chem. B* **2005**, *109*, 17467−17473.

(41) Bao, H. F.; Wang, E. K.; Dong, S. J. One-Pot Synthesis of CdTe Nanocrystals and Shape Control of Luminescent CdTe-Cystine Nanocomposites. *Small* **2006**, *2*, 476−480.

(42) Rajh, T.; Mićić, O. I.; Nozik, A. J. Synthesis and Characterization of Surface-Modified Colloidal CdTe Quantum Dots. *J. Phys. Chem.* **1993**, *97*, 11999−12003.

(43) Gaponik, N.; Talapin, D. V.; Rogach, A. L.; Hoppe, K.; Shevchenko, E. V.; Kornowski, A.; Eychmüller, A.; Weller, H. Thiol-Capping of CdTe Nanocrystals: An Alternative to Organometallic Synthetic Routes. *J. Phys. Chem. B* **2002**, *106*, 7177−7185.

(44) Qian, H. F.; Dong, C. Q.; Weng, J. F.; Ren, J. C. Facile One-Pot Synthesis of Luminescent, Water-Soluble, and Biocompatible Gluta-thione-Coated CdTe Nanocrystals. *Small* **2006**, *2*, 747−751.

(45) Green, M.; Harwood, H.; Barrowman, C.; Rahman, P.; Eggeman, A.; Festry, F.; Dobson, P.; Ng, T. A Facile Route to CdTe Nanoparticles and Their Use in Bio-Labelling. *J. Mater. Chem.* **2007**, *17*, 1989−1994.

(46) He, Y.; Sai, L. M.; Lu, H. T.; Hu, M.; Lai, W. Y.; Fan, Q. L.; Wang, L. H.; Huang, W. Microwave-Assisted Synthesis of Water-Dispersed CdTe Nanocrystals with High Luminescent Efficiency and Narrow Size Distribution. *Chem. Mater.* **2007**, *19*, 359−365.

(47) Sgobba, V.; Schulz-Drost, C.; Guldi, D. M. Synthesis and Characterization of Positively Capped CdTe Quantum Wires That Exhibit Strong Luminescence in Aqueous Media. *Chem. Commun.* **2007**, 565−567.

(48) Wang, Z. Y.; Zong, S. F.; Li, W.; Wang, C. L.; Xu, S. H.; Chen, H.; Cui, Y. P. SERS-Fluorescence Joint Spectral Encoding Using Organic-Metal-QD Hybrid Nanoparticles with a Huge Encoding Capacity for High-Throughput Biodetection: Putting Theory into Practice. *J. Am. Chem. Soc.* **2012**, *134*, 2993−3000.

(49) Mamedov, A. A.; Belov, A.; Giersig, M.; Mamedova, N. N.; Kotov, N. A. Nanorainbows: Graded Semiconductor Films from Quantum Dots. *J. Am. Chem. Soc.* **2001**, *123*, 7738−7739.

(50) Qi, H. S.; Chang, C. Y.; Zhang, L. N. Properties and Applications of Biodegradable Transparent and Photoluminescent Cellulose Films Prepared *via* a Green Process. *Green Chem.* **2009**, *11*, 177−184.

(51) Fu, F. Y.; Li, L. Y.; Liu, L. J.; Cai, J.; Zhang, Y. P.; Zhou, J. P.; Zhang, L. N. Construction of Cellulose Based ZnO Nanocomposite Films with Antibacterial Properties through One-Step Coagulation. *ACS Appl. Mater. Interfaces* **2015**, *7*, 2597−2606.

(52) Talapin, D. V.; Rogach, A. L.; Shevchenko, E. V.; Kornowski, A.; Haase, M.; Weller, H. Dynamic Distribution of Growth Rates within the Ensembles of Colloidal II-VI and III-V Semiconductor Nanocrystals as a Factor Governing Their Photoluminescence Efficiency. *J. Am. Chem. Soc.* **2002**, *124*, 5782−5790.

(53) Aldana, J.; Wang, Y. A.; Peng, X. G. Photochemical Instability of CdSe Nanocrystals Coated by Hydrophilic Thiols. *J. Am. Chem. Soc.* **2001**, *123*, 8844−8850.

(54) Jeong, S.; Achermann, M.; Nanda, J.; Ivanov, S.; Klimov, V. I.; Hollingsworth, J. A. Effect of the Thiol-Thiolate Equilibrium on the Photophysical Properties of Aqueous CdSe/ZnS Nanocrystal Quantum Dots. *J. Am. Chem. Soc.* **2005**, *127*, 10126−10127.

(55) Wang, C. L.; Zhang, H.; Zhang, J. H.; Lv, N.; Li, M. J.; Sun, H. Z.; Yang, B. Ligand Dynamics of Aqueous CdTe Nanocrystals at Room Temperature. *J. Phys. Chem. C* **2008**, *112*, 6330−6336.

(56) Bao, H. B.; Gong, Y. J.; Li, Z.; Gao, M. Y. Enhancement Effect of Illumination on the Photoluminescence of Water-Soluble CdTe Nanocrystals: Toward Highly Fluorescent CdTe/CdS Core-Shell Structure. *Chem. Mater.* **2004**, *16*, 3853−3859.

(57) Zhang, H.; Wang, D. Y.; Yang, B.; Möhwald, H. Manipulation of Aqueous Growth of CdTe Nanocrystals to Fabricate Colloidally Stable One-Dimensional Nanostructures. *J. Am. Chem. Soc.* **2006**, *128*, 10171−10180.

(58) Zhang, H.; Liu, Y.; Wang, C. L.; Zhang, J. H.; Sun, H. Z.; Li, M. J.; Yang, B. Directing the Growth of Semiconductor Nanocrystals in Aqueous Solution: Role of Electrostatics. *ChemPhysChem* **2008**, *9*, 1309−1316.

(59) Nair, P. V.; Thomas, K. G. Hydrazine-Induced Room-Temperature Transformation of CdTe Nanoparticles to Nanowires. *J. Phys. Chem. Lett.* **2010**, *1*, 2094−2098.

(60) Zhou, D.; Liu, M.; Lin, M.; Bu, X. Y.; Luo, X. T.; Zhang, H.; Yang, B. Hydrazine-Mediated Construction of Nanocrystal Self-Assembly Materials. *ACS Nano* **2014**, *8*, 10569−10581.

(61) Zhang, H.; Wang, C. L.; Li, M. J.; Ji, X. L.; Zhang, J. H.; Yang, B. Fluorescent Nanocrystal-Polymer Composites from Aqueous Nano-crystals: Methods without Ligand Exchange. *Chem. Mater.* **2005**, *17*, 4783−4788.

(62) Zhang, H.; Zhou, Z.; Yang, B.; Gao, M. Y. The Influence of Carboxyl Groups on the Photoluminescence of Mercaptocarboxylic Acid-Stabilized CdTe Nanoparticles. *J. Phys. Chem. B* **2003**, *107*, 8−13.